Cell Reports

Dorsal Premotor Cortex Neurons Signal the Level of Choice Difficulty during Logical Decisions

Graphical Abstract

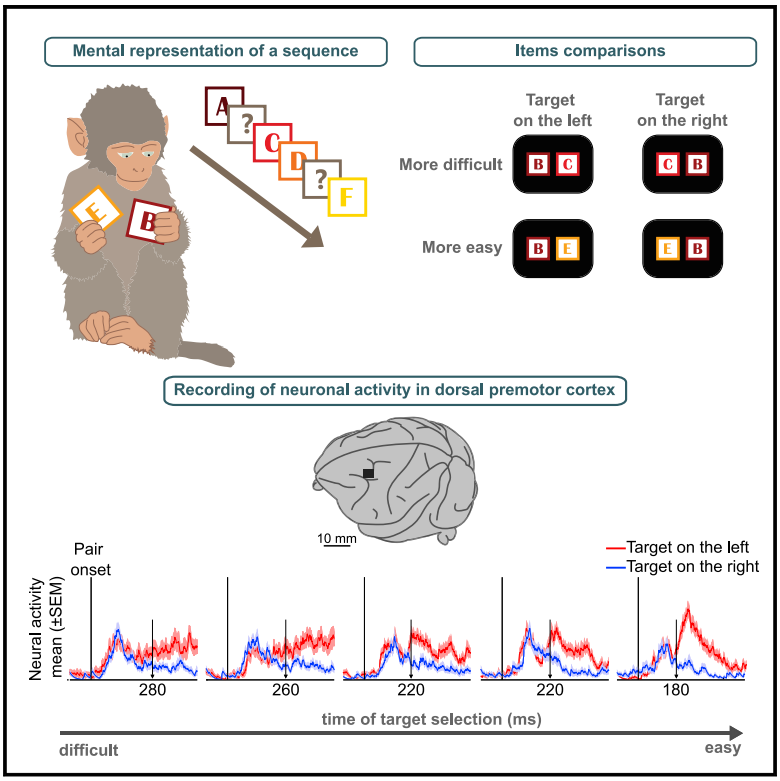

Highlights

- Monkeys were trained in rank ordering a set of items to form a mental representation
- Performance suggests the use of a mental model to map learned premises
- Discrimination is more difficult for items close in ranks in the mental model
- Premotor cortex neurons' modulation reflects levels of difficulty

Authors

Valentina Mione, Emiliano Brunamonti, Pierpaolo Pani, Aldo Genovesio, Stefano Ferraina

Correspondence

emiliano.brunamonti@uniroma1.it

In Brief

Mione et al. show that the degree of discriminability between pairs of rank-ordered items stored in memory (a mental map) modulates neuronal activity in premotor cortex of monkeys with mechanisms comparable with those observed in perceptual decision-making tasks.

Mione et al., 2020, Cell Reports *32*, 107961
July 28, 2020
https://doi.org/10.1016/j.celrep.2020.107961

Cell Reports

CellPress
OPEN ACCESS

Report

Dorsal Premotor Cortex Neurons Signal the Level of Choice Difficulty during Logical Decisions

Valentina Mione,[1] Emiliano Brunamonti,[1,3,*] Pierpaolo Pani,[1] Aldo Genovesio,[1] and Stefano Ferraina[1,2]
[1]Department of Physiology and Pharmacology, Sapienza University, 00185 Rome, Italy
[2]Senior author
[3]Lead Contact
*Correspondence: emiliano.brunamonti@uniroma1.it
https://doi.org/10.1016/j.celrep.2020.107961

SUMMARY

Studies on the neuronal correlates of decision making have demonstrated that the continuous flow of sensorial information is integrated by sensorimotor brain areas in order to select one among simultaneously represented targets and potential actions. In contrast, little is known about how these areas integrate memory information to lead to similar decisions. Using serial order learning, we explore how fragments of information, learned and stored independently (e.g., A > B and B > C), are linked in an abstract representation according to their reciprocal relations (such as A > B > C) and how this representation can be accessed and manipulated to make decisions. We show that manipulating information after learning occurs with increased difficulty as logical relationships get closer in the mental map and that the activity of neurons in the dorsal premotor cortex (PMd) encodes the difficulty level during target selection for motor decision making at the single-neuron and population levels.

INTRODUCTION

The difficulty in detecting the correct choice can influence decision making at various stages, from perception to action, rendering it dependent on the sensory outcome, rule uncertainty, past experience, and inference of the current state (Bach and Dolan, 2012; Genovesio and Ferraina, 2014).

When a forward soccer player sees a team member close to the opposing goal and available for a pass, the decision whether to pass the ball is biased by acquired knowledge on both the player's own ability to score points and its comparison with those of other available members in similar positions. This and many other context-guided decisions rely more on a mental model (i.e., the internal representation of experienced information) than on perceptual information (such as the physical positions of the team members).

Manipulating perceptual (sensory) ambiguity in neurophysiological paradigms in monkeys has advanced our understanding of the neuronal correlates of target detection and decision making in several areas of the brain. In these paradigms, subjects are asked to identify a target item among a set of distractors (Basso and Wurtz, 1997; Schall and Hanes, 1993) or detect one of two potential targets by decoding the directional flow of a set of moving dots (Shadlen and Newsome, 1996) or the instruction that is provided by additional cues (Cisek and Kalaska, 2005). Frontal and parietal brain areas, which are involved in visuomotor transformation and decision making, have typically shown neuronal ramping toward a threshold, whose slope is modulated by the degree of the subject's confidence in identifying the more reliable option among the alternatives (Gold and Shadlen, 2007; Kiani and Shadlen, 2009).

However, we do not have a similar deep understanding of the neural processes taking place when decisions are influenced by internally stored information on the basis of previous experience.

A well-studied instance of this condition is when human subjects are asked to compare numerical quantities. In this case, the decision-making process is based on the mental number line: indeed, subjects typically display a symbolic distance (SDist) effect; that is, their performance is always better for numbers (information) well spaced apart than for those that are close to each other (Moyer and Landauer, 1967), somehow represented in overlapping positions throughout the number line.

Decision making driven by mental models has been also hypothesized to modulate performance in the transitive inference (TI) task (Brunamonti et al., 2011, 2016; Jensen, 2017). In this task, subjects learn premises that A > B, B > C, C > D, D > E, and E > F and then create a mental map, such as A > B > C > D > E > F. This map is used to decide about questions that require a choice between never experienced pairs of items, such as which is higher in value between B and D. A proof of the existence of a mental map in TI is the observation of the well-documented SDist effect, which is thought to reflect the difficulty in detecting the differences between the mental representation of premises, as observed when quantities are compared in mental lines (Brunamonti et al., 2011; Nieder and Dehaene, 2009). More in detail, behavioral performance decreases as the position of the items to compare gets closer in the mental representation; for example, a subject will find it more difficult to choose the higher in value between C and D than between B and D.

In this study, we exploited the TI task to explore the neuronal correlates of decision making on the basis of mental

representations in the dorsal premotor cortex (PMd) of non-human primates. PMd neurons are typically modulated in diverse periods of behavioral tasks, from target representation to decision making (Chandrasekaran et al., 2017; Thura and Cisek, 2014), motor planning, and execution (Caminiti et al., 1991; Weinrich and Wise, 1982). Furthermore, neurons in PMd are modulated by the memory of recent events (Marcos et al., 2013), and studies in humans suggest that this region is involved in logical problem solving in TI tasks (Acuna et al., 2002; Wertheim and Ragni, 2018).

Here we provide evidence that the activity of PMd neurons reflects performance at both the single-neuron and population levels when animals use internal information to contribute to the decision-making process. At the single-neuron level, as the difficulty of a choice between targets increases, fewer neurons are able to provide sufficient information, and the latency to discriminate increases. We found similar results representing population activity in a multi-dimensional space, where neuronal trajectories start to diverge at different times according to the SDist between the compared items, thus signaling the difficulty of the decision.

RESULTS

Choice Difficulty Modulates the Identification of the Target Location during Logical Decision Making

Both monkeys performed daily a TI task with six novel items hierarchically organized (Figures 1A and 1B). In the test phase of the task (see STAR Methods), all pairs of symbols (corresponding to all possible SDists) were presented. In all sessions with simultaneous recording of neuronal activity (monkey 1, n = 7; monkey 2, n = 7), the SDist effect characterized the behavior, suggesting the use of the mental model to map learned premises (see STAR Methods; Figure S1) and a variable choice difficulty. Figures 1C and 1D show that the proportion of correct choices increased and that the reaction time (RT; computed as the time from go signal to movement onset; see Figure 1B) decreased as SDist increased. Of relevance, the most difficult comparison was found for pairs of symbols at SDist 1; conversely, SDist 4 and 5 comparisons were easily managed by both monkeys.

The quantitative analysis of the behavioral outcome revealed that SDist linearly modulated the performance of both monkeys (see Table S1 for details).

Choice Difficulty Is Reflected in the Selectivity of Single-Neuron Activity

We studied 186 PMd-isolated neurons (59 from monkey 1 and 127 from monkey 2; Figure 2A; STAR Methods) during the test phase of the TI task to evaluate how neuronal activity during logical decision making was modulated by the difficulty in selecting the target from the non-target.

The first level of analysis assessed the neuronal population target/action selectivity. We found that the activity of 62% (115 of 186; 45 in monkey 1, 70 in monkey 2) of all recorded neurons differed significantly ($p < 0.001$, t test with Bonferroni correction) for target position/movement direction (right/left, independent of correctness) during the early period after the presentation of the pair (Pair-on) and/or at the time preceding the onset of the movement (Mov-on) (see STAR Methods for more details).

These neurons represented our database. Initially, we studied if SDist modulated their directional activity while the monkeys compared pairs of symbols.

Figure 2B shows the time course of the neuronal activity for the different SDists, aligned to the time of pair presentation, in a neuron of our sample. This neuron displays selectivity for the left target modulated by the choice difficulty. The left target selection (i.e., the directionality) emerged at earlier times and with increasing intensity as choice difficulty decreased (i.e., from comparisons at smaller to higher SDists) well before the go signal (900 ms represents the average duration of the delay; see STAR Methods).

For each of the 115 neurons, we calculated the time course of the differences in activity (expressed as receiver operating characteristic [ROC] values) across correct trials at each SDist and up to 800 ms following the presentation of the target (Figure 2C). ROC values, computed every 20 ms, were used to estimate the time at which each neuron started to encode the target position, defined as the time bin at which the ROC value exceeded 0.6 (encoding, as preferred, the left target position) or fell below 0.4 (encoding, as preferred, the right target position) for three consecutive bins.

The analysis shows that the spatial preference was distributed similarly across the population of neurons, wherein 42% of the cells (48 of 115) preferred the target when on the left of the screen (red traces), compared with the remaining 58% (67 of 115) preferring it when on the right (blue traces). However, the number of cells encoding the target position was highest (n = 82) for pairs with an SDist of 5 (easy to discriminate, on the basis of our behavioral analysis) and decreased as the SDist declined (SDist 1, n = 52). Moreover, the start of significant selectivity (white dots) was delayed in all SDists compared with SDist 5. The median time (vertical arrows in Figure 2C) at which the population of neurons significantly encoded the target increased gradually from SDist 5 to SDist 1 ($p < 0.001$, Kruskal-Wallis test), always anticipating the go signal. Finally, the average magnitude of discrimination (ROC value) across neurons in the 800 ms following the target onset was significantly higher at SDist 5 than at lower SDists (average area under the ROC curve [AuROC]: SDist 1 = 0.52 [SEM = 0.008], SDist 2 = 0.52 [SEM = 0.010], SDist 3 = 0.54 [SEM = 0.009], SDist 4 = 0.53 [SEM = 0.008], SDist 5 = 0.56 [SEM = 0.008]; $p < 0.001$, Kruskal-Wallis test).

Considering the different number of selective neurons in the different SDists, we investigated a possible categorical representation of difficulty. We detected that 32 of 82 neurons (39%) displayed selectivity for all SDists. A small percentage (11 of 82 [13%]) showed selectivity only for SDist ≥ 3, suggesting the possibility of a categorical representation of more easy comparisons in these neurons. The remaining 39 of 82 (48%) showed a more complex representation based on the lack of sensitivity in at least one SDist (other than SDist 5, always present). A similar result was evident when considering the distribution of discrimination times among neurons (not shown).

Overall, these results demonstrate that PMd activity reflected better the target choice when the ranks of the symbols were easy to discriminate and suggest that target selection is subtended by complex interactions among all neurons.

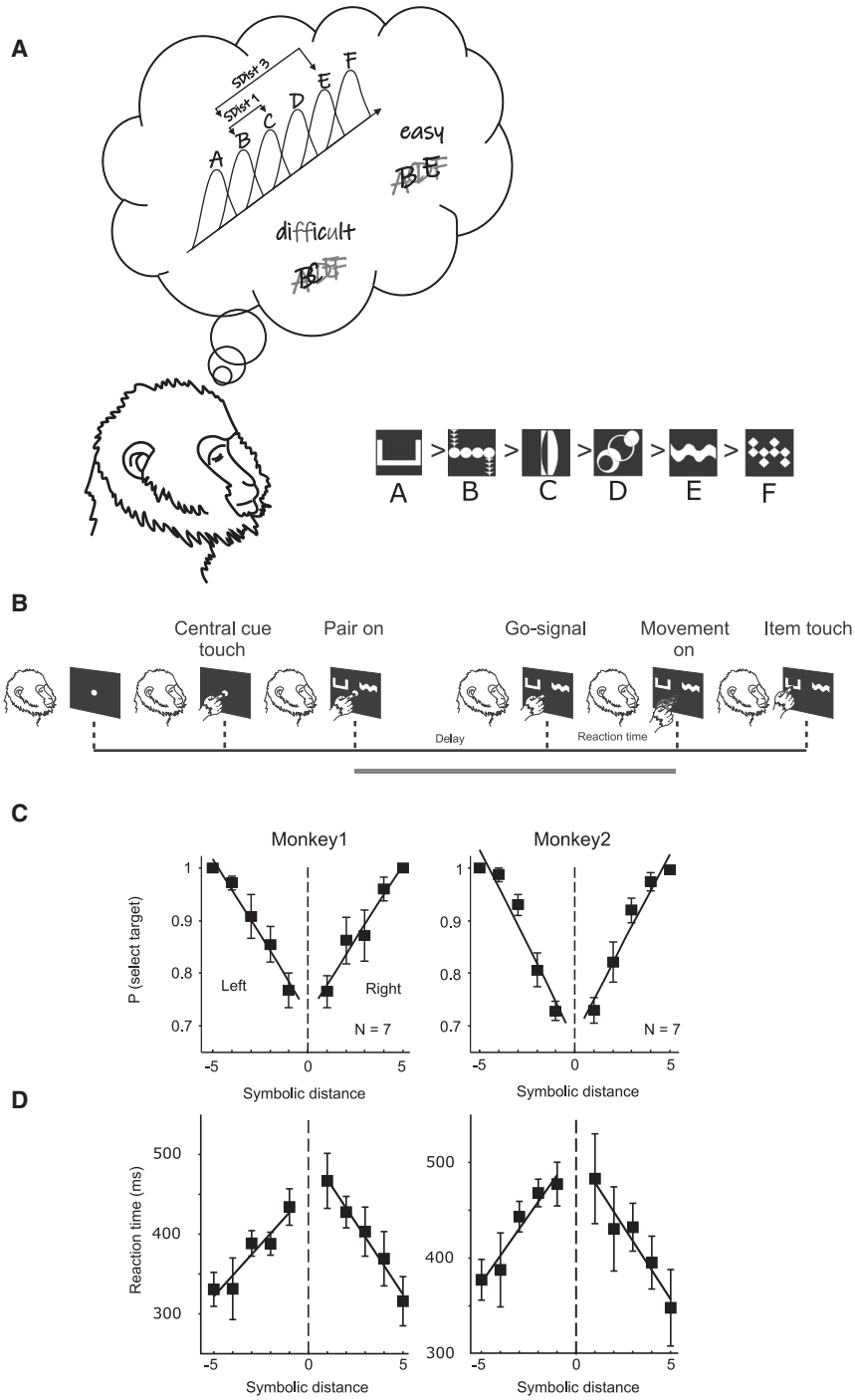

Figure 1. Experimental Task and Behavioral Performance

(A) Schematic of the hypothesized mental representation of the rank-ordered items acquired after the learning procedures. Choice difficulty is represented as a function of the degree of overlap between adjacent and spaced pairs of items in the series. A sample series used in the experiment is displayed.

(B) Time course of the experimental task in the test phase (after learning). Monkeys were required to wait for the presentation of a pair of items while they touched a white dot at the center of a touch-sensitive computer screen. After, the central dot disappeared (go signal), instructing the monkeys to touch the selected item on the screen. The choice of the higher ranked item in the pair, according to the series in (A), was rewarded. The dark gray line indicates the epoch of neuronal analysis.

(C and D) Average performance and RTs of the two monkeys with regard to the spatial position of the target and the SDist: (C) proportion of correct selections of target when presented on the right and left position is reported; (D) reaction time. They both showed an increasing tendency to choose more accurately the target from the non-target as the SDist increased. Error bars in (C) and (D) indicate SEM.

Population Encoding of Target Position under Different Degrees of Difficulty

To examine the neuronal mechanisms at the population level, we used principal-component analysis (PCA) and trajectories for representing the changes of activity in the functional state space during target selection and, consequently, logical decision making. We used the first 15 principal components (PCs) as the reference frame, accounting for 82% of the variability in the neuronal activity of monkey 1 and 88% of that of monkey 2.

Figures 3A and 3B show, for illustrative purposes, the temporal evolution of the neuronal activity during the comparison of items for each monkey as trajectories in a system formed by the first 3 PCs. Neuronal trajectories are shown for all trials that corresponded to the same spatial selection (left or right; thicker red and blue lines) and for trials that corresponded to various conditions, sorted by SDist (thinner lines). The neuronal trajectories of both animals began to diverge toward the neuronal state that corresponded to the decision, long before the presentation of the go signal (triangle). As evidence of this separation, Figures 3C and 3D show that the Euclidean distance between trajectories (computed for each SDist on the first 15 PCs) increased with increasing latency, in agreement with difficulty, displaying a gradual ordered organization on both animals (vertical arrows; even with animal-specific characteristics). On average, the Euclidean distance exceeded the value that was calculated in the control time (120 ms around the target presentation) at 180 and 600 ms after the target presentation in monkeys 1 and 2, respectively, by more than 3.5 SDs. These times preceded the time of the go signal (shaded lines in Figures 3C and 3D) by 620 ms in monkey 1 and 300 ms

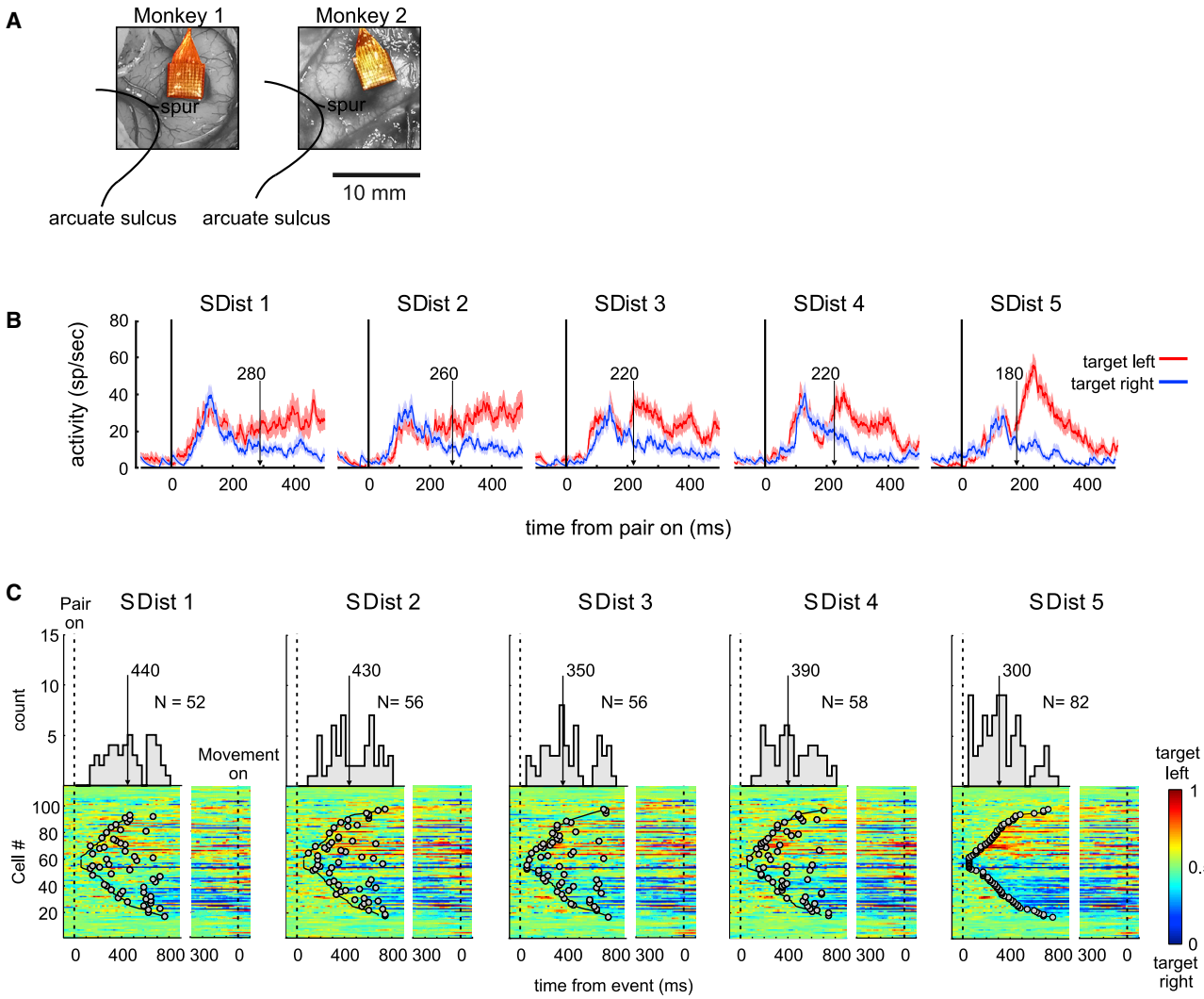

Figure 2. Single-Neuron Activity in TI Task and Color Map of ROC Values for Overall Neuronal Sample

(A) Location of recording array in both monkeys in relation to the approximate location of the arcuate sulcus and spur of the arcuate.

(B) Mean spike density function (shading denotes SEM) of the time course of neuronal activity for left (red) and right (blue) targets for each SDist at the time around the pair presentation.

(C) Time course of ROC values from 100 ms before to 800 ms after the target onset (leftmost plot for each SDist) and 400 ms before to 100 ms after the onset of movement (rightmost plot). Neurons are sorted according to their degree of discrimination of the target location at SDist 5 in the 800 ms following the pair onset. The same order overall was kept for the other SDists for both epochs. Gray points in the map highlight each time bin passing the criterion of ROC value > 0.6 and ROC < 0.4. Histograms show discrimination time at each SDist for the first epoch of analysis together with the median discrimination time (arrows) and the number of neurons reaching the discrimination criteria.

in monkey 2. By comparing the two extreme cases, we observed that the trajectories for the comparisons at SDist 5 reached significance about 340 and 120 ms before the comparisons at SDist 1 in monkey 1 and monkey 2, respectively.

The difference in time of target detection for the two animals suggests that the process is not terminated after discrimination. In fact, the RT range is very similar in the two animals (see Figure 1D). To detect further modulations after the time each trajectory passed the relative threshold, we computed a measure of the total displacement, before movement onset, by using the cumulative sum of the velocity for each SDist and monkey, separate for the two directions of movements. We performed this analysis after having assessed that the compared trajectories did not deviate significantly from a parallel pathway in all 15 dimensions (as suggested by the first three PCs; Figures 3A and 3B). To this end, we analyzed the degree of parallelism of all pairs of trajectories in 15 dimensions (see STAR Methods). Our analysis revealed no significant differences ($p > 0.01$ for all, Bonferroni post hoc test) with an overall lack of significant deviation of the SDist trajectories from a parallel pathway in the epoch of analysis.

Figure 4 shows the cumulative sum (i.e., the final total displacement) differentiated in an ordered manner according to

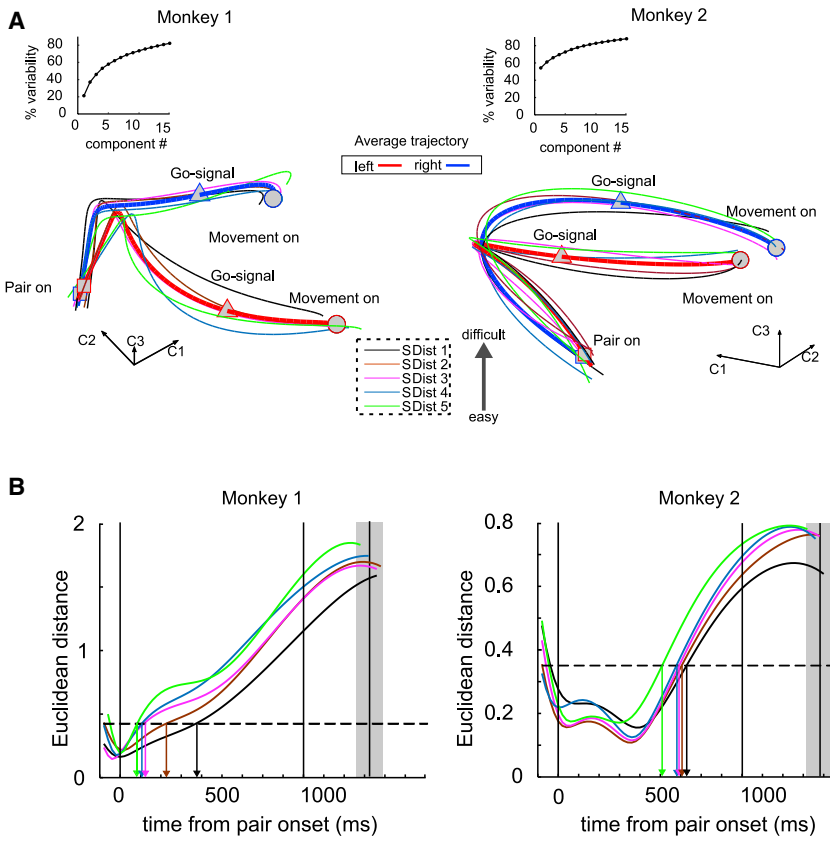

Figure 3. Network Dynamics of Decision Making during the TI Task

(A) Neuronal trajectory of the decision process in both monkeys during TI is represented in a tridimensional state space, when the target was located on the left (red tick line) and right (blue thick line). Thin colored lines represent the decision process at different SDists. The decision process is tracked from the 100 ms preceding the presentation of the pair of items (squares) to the time of movement onset (circles), after the presentation of the go signal (triangles).

(B) Time course of Euclidean distance between trajectories, for the left and right targets, for both monkeys as in (A). The dotted horizontal line indicates the threshold used to mark the time at which the average left and right trajectories begin to separate significantly; the exact time for each SDist is marked with an arrow colored accordingly. Vertical black solid lines indicate the pair onset (at time 0) and average go signal, respectively. Shaded gray vertical bar highlights the movement onset time (mean ± 1 SD).

the differences in SDists during its increase. We found that once the position of the target was identified at the neuronal level (threshold in Figure 3), the state that corresponded to the onset of movement (colored circles) was attained more rapidly for the easiest comparisons at SDist 5 than for more difficult comparisons at lower distances. The slope of the cumulative sum of the velocity for both target positions resulted significantly steeper (by analysis of covariance [ANCOVA]) for higher versus smaller SDist and similar in both monkeys (see Table S1).

We obtained comparable results in the state space analysis by considering either only sessions in which monkeys acquired the mental representation of the items' rank by the chain-linking learning procedure (see STAR Methods; Figure S1A; Figure S2) or only SDist-modulated neurons, as highlighted by the ROC analysis (Figure S4).

It is worth noticing that we performed the PCA on all isolated neurons (n = 186) and included both correct and error trials. By this approach, we tested the power of the state space analysis to capture the signals relevant for completing the task in presence of complex interaction between neurons, including those excluded by criteria relaying on standard single-unit statistics.

Overall, these results suggest that the discriminability of the target position and the consequent decision are reflected in the dynamic of the network activity. Specifically, we observed that the neuronal trajectory dynamics were strongly influenced by target discriminability and decision-making difficulty.

DISCUSSION

We used a TI task to investigate the neuronal correlates of decision making on the basis of internal (mental) representations. We instructed two macaque monkeys to select between pairs of targets, on the basis of an ordered rank learned during a previous trial-and-error training session.

We found that the closer the ranks, the more difficult the decision processes, as observed in the decline in correct choices and in the increasing RTs. Importantly, the neural activity of PMd neurons reflected these behavioral effects; indeed, neuronal activity was differently modulated in conditions in which the choice was easy because of a large SDist between targets, compared with conditions in which the choice was difficult because of a small SDist and, presumably, a higher degree of overlap between two stimuli in the mental schema formed during serial learning.

We recognized two neuronal mechanisms in the PMd that correlated with the difficulty of the decision: (1) as the difficulty in discriminating the target decreased, more neurons were recruited, and (2) the decline in difficulty was accompanied by a shorter neuronal discrimination latency.

Comparing Paradigms: Mental Schema-Driven versus Perceptually Driven Decision Making

The neuronal correlates of decision making have been studied widely using perceptual decision-making tasks. The commonly used task design requires to identify a target item or its location by comparing its static or dynamic visual features among a set of distractors (Basso and Wurtz, 1997; Coallier et al., 2015; Hanks and Summerfield, 2017). By manipulating the degree of perceptual overlap between a target and distractors, researchers have

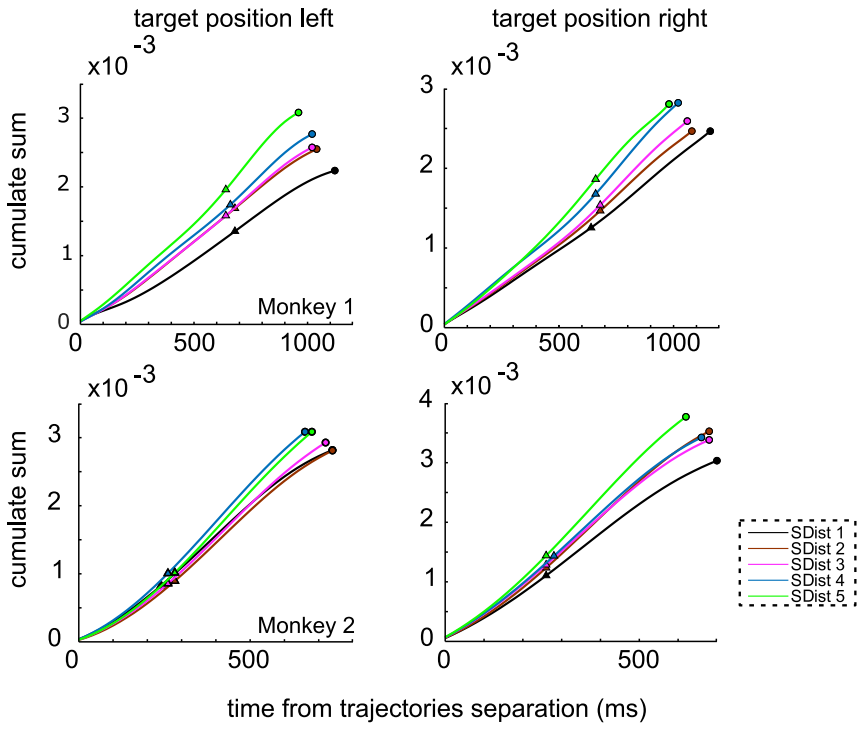

Figure 4. Network Dynamics from the Neuronal Response Time to Movement Onset

Cumulative sum of instant velocity from the time of trajectory separation to the onset of movement (colored circles) for left and right target locations and different SDists for both monkeys. Colored triangles mark the time of the go signal. The slope of the lines indicates that the dynamics are faster (short RT) for greater SDist.

modulated the perceptual uncertainty and correlated the activity of several sensorimotor areas to this process (Hanks and Summerfield, 2017). The main finding of these studies has been to highlight a difference in the ramp-up toward a threshold of neuronal activity. This process has been modeled by dynamic competition between mutually inhibitory units that increase their response as the incoming perceptual information favors one of the options (Smith and Ratcliff, 2004; Wang, 2002). In motor areas, this competition has been related to the selection of the more reliable action among a set of actions that are simultaneously represented in an ambiguous context (Cisek and Kalaska, 2010), and perceptual decision making is viewed as a means of selecting the more appropriate motor action (Cisek and Kalaska, 2010; Shushruth et al., 2018).

We have shown that the ambiguity in mental representation influences the neuronal correlates of a commitment to an action in motor areas. Also, we addressed whether two decision processes share some features (Shadlen and Shohamy, 2016). In our paradigm, a given stimulus corresponded to the target or distractor (non-target), depending on its position in the mental map, as acquired during the serial learning training. Thus, perceptual identification of the item is insufficient for making a decision without accessing the mental representation of the serially ordered items. In this scenario, perceptual information serves only as link between the stimulus and its abstract representation in the mental map that drives the response.

We observed that the rank/distance (SDist) of the memorized items in the hierarchically organized mental map—a manipulation of the signal-to-noise ratio in target detection—altered the performance and modulated neurons at the single-cell and population levels. In fact, the decrease in the overlap between target and non-target in the mental schema improved the performance, increased the number of neurons that were selective for the target, and anticipated the time of logical target selection. Similar behavioral and neuronal correlates have been observed in the perceptual decision tasks, in which the coherence of moving dots (Hanks and Summerfield, 2017), the proportion of colored dots (Coallier et al., 2015), the proportion of distracting items (Basso and Wurtz, 1997; Schall and Hanes, 1993), and visual salience (Pani et al., 2018; Shen et al., 2010) are manipulated.

The study of the network dynamic as a moving point in a multi-dimensional space revealed that choice difficulty in committing to an action influenced the evolution of the network dynamic toward a decision state, with the timing depending on the difficulty of the decision and the degree of certainty.

Our results are consistent with the simultaneous representation of potential multiple actions in motor areas (Cisek and Kalaska, 2010). In our approach, we presented two potential targets of action simultaneously. By relying on their mental representation, suggested to be encoded in the prefrontal cortex (Brunamonti et al., 2016), the monkeys were required to indicate whether the target was on the left or right and activate a motor plan to reach it. We showed that neuronal trajectories for reaching leftward and rightward overlapped after the presentation of the two stimuli and then diverged, depending on the target position that was identified. The divergence between neural trajectories occurred approximately 200–600 ms after presentation of the pair, timing that is compatible with that reported in earlier studies in which selection was required by simple (Cisek and Kalaska, 2005) or complex static stimuli (Chandrasekaran et al., 2017; Coallier et al., 2015) or dynamically changing stimuli (Thura and Cisek, 2014). These results are also consistent with the competition between groups of units, representing different outcomes (Wang, 2002) and gradually becoming more responsible for target selection as the decision evolves over time (Cisek and Kalaska, 2005).

Function of the PMd in Abstract Tasks

The PMd is engaged in a wide range of highly abstract reasoning tasks (Abe and Hanakawa, 2009; Goel and Dolan, 2004; Hanakawa et al., 2002; Tanaka et al., 2005, 2015), including the

representation of abstract information and rules (Wallis and Miller, 2003), even when actions are not performed directly (Cirillo et al., 2018; Cisek and Kalaska, 2004). Neuroimaging studies have demonstrated that this brain area is active in humans who perform a TI task (Wertheim and Ragni, 2018), but they lack details on the neuronal mechanisms. In several neuroimaging and neurophysiology studies (Acuna et al., 2002; Ohbayashi et al., 2003), the premotor cortex in human and monkeys is recruited every time sequential information is generated and when previously unrelated elements must be integrated into a sequence, increasing our understanding of its function in the TI task. These activities reflect the fundamental role of the PMd in conditional visuomotor association, especially in the representation and integration of relevant abstract information, on the basis of visual stimuli that are necessary to specify goal-directed actions (for reviews, see Amiez et al., 2006; Hoshi, 2013).

The neuronal dynamic we observed indeed fulfills the requirements of being selective well before movement onset and being influenced by the decision variables (Padoa-Schioppa, 2011; Thura and Cisek, 2014), consistent with an active role of PMd in decision making.

The profile of the PMd described so far, together with the overall results and this latest evidence, support the hypothesis that PMd functions in processing internal information that leads to decision making and that this activity is not simply a reflection of the computation of these decision processes.

Our results show that PMd takes part in the discrimination of the two symbols used for each test, well before the movement is planned and executed. Because animals were well aware that any response before the go signal corresponded to an aborted trial and a lack of reward, we assume that a committed state is delayed in the following interval. We tentatively speculate that because of the task construction, the committed state requires an external source (or additional signal) to remove the inhibition. However, our task cannot solve the issue, and we are aware that such a result is not incompatible with the alternative hypothesis that PMd is more involved in manipulating choice representation in order to generate a final motor plan, receiving information from upstream areas.

STAR★METHODS

Detailed methods are provided in the online version of this paper and include the following:

- KEY RESOURCE TABLE
- RESOURCE AVAILABILITY
  - Lead Contact
  - Materials availability
  - Data and Code Availability
- EXPERIMENTAL MODEL AND SUBJECT DETAILS
- METHOD DETAILS
  - Subjects and recording apparatus
  - Test stimuli and task design
- QUANTIFICATION AND STATISTICAL ANALYSIS
  - Behavioral data
  - Neural data
  - Population analysis using PCA

SUPPLEMENTAL INFORMATION

Supplemental Information can be found online at https://doi.org/10.1016/j.celrep.2020.107961.

ACKNOWLEDGMENTS

This study was partially supported by Sapienza University grants PH11715C823A9528, PH1181642DB714F6, and RP11715C7E0BBC4A and European Commission (EC) grant FET 306502. We would like to thank Dr. Valeria Fascinelli, Giampiero Bardella, and Andrea Ciardiello for their support for the data reduction analysis.

AUTHOR CONTRIBUTIONS

E.B. and S.F. designed research. V.M. performed research. V.M. and E.B. analyzed data. All authors discussed and interpreted the results. V.M., E.B., and S.F. wrote the paper.

DECLARATION OF INTERESTS

The authors declare no competing interests.

Received: July 23, 2019
Revised: April 7, 2020
Accepted: July 2, 2020
Published: July 28, 2020

REFERENCES

Abe, M., and Hanakawa, T. (2009). Functional coupling underlying motor and cognitive functions of the dorsal premotor cortex. Behav. Brain Res. *198*, 13–23.

Acuna, B.D., Eliassen, J.C., Donoghue, J.P., and Sanes, J.N. (2002). Frontal and parietal lobe activation during transitive inference in humans. Cereb. Cortex *12*, 1312–1321.

Amiez, C., Kostopoulos, P., Champod, A.-S., and Petrides, M. (2006). Local morphology predicts functional organization of the dorsal premotor region in the human brain. J. Neurosci. *26*, 2724–2731.

Bach, D.R., and Dolan, R.J. (2012). Knowing how much you don't know: a neural organization of uncertainty estimates. Nat. Rev. Neurosci. *13*, 572–586.

Basso, M.A., and Wurtz, R.H. (1997). Modulation of neuronal activity by target uncertainty. Nature *389*, 66–69.

Brunamonti, E., Genovesio, A., Carbè, K., and Ferraina, S. (2011). Gaze modulates non-propositional reasoning: further evidence for spatial representation of reasoning premises. Neuroscience *173*, 110–115.

Brunamonti, E., Mione, V., Di Bello, F., De Luna, P., Genovesio, A., and Ferraina, S. (2014). The NMDAr antagonist ketamine interferes with manipulation of information for transitive inference reasoning in non-human primates. J. Psychopharmacol. (Oxford) *28*, 881–887.

Brunamonti, E., Mione, V., Di Bello, F., Pani, P., Genovesio, A., and Ferraina, S. (2016). Neuronal modulation in the prefrontal cortex in a transitive inference task: evidence of neuronal correlates of mental schema management. J. Neurosci. *36*, 1223–1236.

Caminiti, R., Johnson, P.B., Galli, C., Ferraina, S., and Burnod, Y. (1991). Making arm movements within different parts of space: the premotor and motor cortical representation of a coordinate system for reaching to visual targets. J. Neurosci. *11*, 1182–1197.

Chandrasekaran, C., Peixoto, D., Newsome, W.T., and Shenoy, K.V. (2017). Laminar differences in decision-related neural activity in dorsal premotor cortex. Nat. Commun. *8*, 614.

Cirillo, R., Ferrucci, L., Marcos, E., Ferraina, S., and Genovesio, A. (2018). Coding of Self and Other's Future Choices in Dorsal Premotor Cortex during Social Interaction. Cell Rep. *24*, 1679–1686.

Cisek, P., and Kalaska, J.F. (2004). Neural correlates of mental rehearsal in dorsal premotor cortex. Nature *431*, 993–996.

Cisek, P., and Kalaska, J.F. (2005). Neural correlates of reaching decisions in dorsal premotor cortex: specification of multiple direction choices and final selection of action. Neuron *45*, 801–814.

Cisek, P., and Kalaska, J.F. (2010). Neural mechanisms for interacting with a world full of action choices. Annu. Rev. Neurosci. *33*, 269–298.

Coallier, É., Michelet, T., and Kalaska, J.F. (2015). Dorsal premotor cortex: neural correlates of reach target decisions based on a color-location matching rule and conflicting sensory evidence. J. Neurophysiol. *113*, 3543–3573.

Fraser, G.W., and Schwartz, A.B. (2012). Recording from the same neurons chronically in motor cortex. J. Neurophysiol. *107*, 1970–1978.

Genovesio, A., and Ferraina, S. (2014). The influence of recent decisions on future goal selection. Philos. Trans. R. Soc. Lond. B Biol. Sci. *369*, 20130477.

Goel, V., and Dolan, R.J. (2004). Differential involvement of left prefrontal cortex in inductive and deductive reasoning. Cognition *93*, B109–B121.

Gold, J.I., and Shadlen, M.N. (2007). The neural basis of decision making. Annu. Rev. Neurosci. *30*, 535–574.

Hanakawa, T., Honda, M., Sawamoto, N., Okada, T., Yonekura, Y., Fukuyama, H., and Shibasaki, H. (2002). The role of rostral Brodmann area 6 in mental-operation tasks: an integrative neuroimaging approach. Cereb. Cortex *12*, 1157–1170.

Hanks, T.D., and Summerfield, C. (2017). Perceptual decision making in rodents, monkeys, and humans. Neuron *93*, 15–31.

Hoshi, E. (2013). Cortico-basal ganglia networks subserving goal-directed behavior mediated by conditional visuo-goal association. Front. Neural Circuits *7*, 158.

Jensen, G. (2017). Serial learning. In APA Handbook of Comparative Psychology: Perception, Learning, and Cognition, J. Call, G.M. Burghardt, I.M. Pepperberg, C.T. Snowdon, and T. Zentall, eds. (Washington, DC: American Psychological Association).

Kiani, R., and Shadlen, M.N. (2009). Representation of confidence associated with a decision by neurons in the parietal cortex. Science *324*, 759–764.

Marcos, E., Pani, P., Brunamonti, E., Deco, G., Ferraina, S., and Verschure, P. (2013). Neural variability in premotor cortex is modulated by trial history and predicts behavioral performance. Neuron *78*, 249–255.

Moyer, R.S., and Landauer, T.K. (1967). Time required for judgements of numerical inequality. Nature *215*, 1519–1520.

Nieder, A., and Dehaene, S. (2009). Representation of number in the brain. Annu. Rev. Neurosci. *32*, 185–208.

Ohbayashi, M., Ohki, K., and Miyashita, Y. (2003). Conversion of working memory to motor sequence in the monkey premotor cortex. Science *301*, 233–236.

Padoa-Schioppa, C. (2011). Neurobiology of economic choice: a good-based model. Annu. Rev. Neurosci. *34*, 333–359.

Pani, P., Giarrocco, F., Giamundo, M., Montanari, R., Brunamonti, E., and Ferraina, S. (2018). Visual salience of the stop signal affects the neuronal dynamics of controlled inhibition. Sci. Rep. *8*, 14265.

Schall, J.D., and Hanes, D.P. (1993). Neural basis of saccade target selection in frontal eye field during visual search. Nature *366*, 467–469.

Shadlen, M.N., and Newsome, W.T. (1996). Motion perception: seeing and deciding (motion perception/psychophysics/decision making/parietal cortex). Proc. Natl. Acad. Sci. U S A *93*, 628–633.

Shadlen, M.N., and Shohamy, D. (2016). Decision making and sequential sampling from memory. Neuron *90*, 927–939.

Shen, K., Kalwarowsky, S., Clarence, W., Brunamonti, E., and Paré, M. (2010). Beneficial effects of the NMDA antagonist ketamine on decision processes in visual search. J. Neurosci. *30*, 9947–9953.

Shushruth, S., Mazurek, M., and Shadlen, M.N. (2018). Comparison of decision-related signals in sensory and motor preparatory responses of neurons in area LIP. J. Neurosci. *38*, 6350–6365.

Smith, P.L., and Ratcliff, R. (2004). Psychology and neurobiology of simple decisions. Trends Neurosci. *27*, 161–168.

Tanaka, S., Honda, M., and Sadato, N. (2005). Modality-specific cognitive function of medial and lateral human Brodmann area 6. J. Neurosci. *25*, 496–501.

Tanaka, S., Pan, X., Oguchi, M., Taylor, J.E., and Sakagami, M. (2015). Dissociable functions of reward inference in the lateral prefrontal cortex and the striatum. Front. Psychol. *6*, 995.

Thompson, K.G., Hanes, D.P., Bichot, N.P., and Schall, J.D. (1996). Perceptual and motor processing stages identified in the activity of macaque frontal eye field neurons during visual search. J. Neurophysiol. *76*, 4040–4055.

Thura, D., and Cisek, P. (2014). Deliberation and commitment in the premotor and primary motor cortex during dynamic decision making. Neuron *81*, 1401–1416.

Treichler, F.R., and Raghanti, M.A. (2010). Serial list combination by monkeys (Macaca mulatta): test cues and linking. Anim. Cogn. *13*, 121–131.

Treichler, F.R., Raghanti, M.A., and Van Tilburg, D.N. (2003). Linking of serially ordered lists by macaque monkeys (Macaca mulatta): list position influences. J. Exp. Psychol. Anim. Behav. Process. *29*, 211–221.

von Fersen, L., Wynne, C., Delius, J.D., and Staddon, J.E. (1991). Transitive inference formation in pigeons. J. Exp. Psychol. Anim. Behav. Process. *17*, 334–341.

Wallis, J.D., and Miller, E.K. (2003). From rule to response: neuronal processes in the premotor and prefrontal cortex. J. Neurophysiol. *90*, 1790–1806.

Wang, X.-J. (2002). Probabilistic decision making by slow reverberation in cortical circuits. Neuron *36*, 955–968.

Weinrich, M., and Wise, S.P. (1982). The premotor cortex of the monkey. J. Neurosci. *2*, 1329–1345.

Wertheim, J., and Ragni, M. (2018). The neural correlates of relational reasoning: a meta-analysis of 47 functional magnetic resonance studies. J. Cogn. Neurosci. *30*, 1734–1748.

Yu, B.M., Cunningham, J.P., Santhanam, G., Ryu, S.I., Shenoy, K.V., and Sahani, M. (2009). Gaussian-process factor analysis for low-dimensional single-trial analysis of neural population activity. J. Neurophysiol. *102*, 614–635.

STAR★METHODS

KEY RESOURCE TABLE

REAGENT or RESOURCE	SOURCE	IDENTIFIER
Experimental Models: Organisms/Strains		
Primate: Rhesus macaque	Sapienza "University of Rome"	N/A
Software and Algorithms		
Cortex	NIMH Cortex	https://nimh.nih.gov
Off Line Sorter	Plexon Inc	https://plexon.com/
MATLAB	MathWorks	https://www.mathworks.com/
Custom-made data analysis scripts (MATLAB)		N/A
Other		
Neuronal recording RZ2 TDT system	Tucker-Davis Technologies, Alachua, FL, USA	https://www.tdt.com/
96-channel microelectrode array	Blackrock Microsystems, Salt Lake City, Utah	https://www.blackrockmicro.com/electrode-types/utah-array/
Arrington eye-tracker system	Arrington Research, Scottsdale, USA	http://www.arringtonresearch.com/

RESOURCE AVAILABILITY

Lead Contact

Further information and requests for resources should be directed to and will be fulfilled by the Lead Contact Emiliano Brunamonti, emiliano.brunamonti@unitroma1.it.

Materials availability

This study did not generate new unique reagents.

Data and Code Availability

The data supporting the current study have not been deposited in a public repository but are available from the Lead Contact author upon request.

EXPERIMENTAL MODEL AND SUBJECT DETAILS

Two male rhesus monkeys (Macaca mulatta), weighing 10.00 kg (Monkey 1) and 9.00 kg (Monkey 2), were chronically implanted in the left PMd cortex with a 96-channel microelectrode array (Blackrock Microsystems, Salt Lake City, Utah). Animal care, housing, and experimental procedures conformed to European (Directive 2010/63/EU) and Italian (D.L. 26/2014) laws on the use of non-human primates in scientific research. The research protocol was approved by the Italian Health Ministry. The housing conditions and the experimental procedures were in accordance with the recommendations of the Weatherall report (use of non-human primates in research).

METHOD DETAILS

Subjects and recording apparatus

Subjects were chronically implanted in the left PMd cortex with a 96-channel microelectrode array (Blackrock Microsystems, Salt Lake City, Utah). Both monkeys were tested on a TI task while neural activity was recorded extracellularly. All surgical procedures were performed using aseptic techniques under general anesthesia (1%–3% isoflurane/O_2, to effect).

The behavioral task was implemented using the freeware software package Cortex (https://nimh.nih.gov/) to control the visual display for the presentation of stimuli and a touchscreen (MicroTouch, sampling rate of 200 Hz) connected to a PC via a serial port to detect the choice. An RZ2 TDT system (Tucker-Davis Technologies, Alachua, FL, USA) that was synchronized to the behavioral events recorded the neural activity during each behavioral trial, and the eye movements were recorded by an Arrington eye-tracker system (Arrington Research, Scottsdale, USA).

Test stimuli and task design

The monkeys were trained to learn a new rank-ordered sequence of 6 items (Figure 1A) in each session, exploring the reciprocal relationships between pairs of them. The items were chosen from a set of 80 black and white abstract images (bitmaps, 16° x 16° visual angle) and changed every day to avoid task solution based on familiarity (Brunamonti et al., 2014, 2016).

At the beginning of each trial, the monkey was instructed to touch (using the right hand) a red fixation cue at the center of the screen (a red circle 13.5° x 13.5° visual angle) to make a pair of items appear on the screen. After a random waiting time (ranging from 600 to 1200 ms), the disappearance of the fixation cue was the Go-signal to release the touch and choose one of the two items. Only the choice of the item higher in rank (randomly presented to the left or right of the screen midline) was rewarded (Figure 1B).

Each experimental session (7 for Monkey 1 and 7 for Monkey 2) was divided into two different phases: a learning phase, in which the monkeys learned the relationships between the adjacent items only of the series, and a test phase, in which this acquired knowledge was used to solve inferential problems (also including pairs of nonadjacent symbols in the series).

Two different learning procedures were presented: 1) a chain-linking learning procedure (Brunamonti et al., 2016) and 2) a sequential learning procedure.

In the first case, the original 6-item list was split into 2 3-item sequences (Figure S1), learned independently (e.g., **A** versus **B**, then **B** versus **C** in one block**; D** versus **E**, then **E** versus **F** in a different block) until the learning criterion was reached (80% of correct responses), and then linked by training on the **C** versus **D** pair (20 trials block). In the sequential learning procedure, all pair of items with an adjacent rank was presented sequentially in blocks of 20 trials (e.g., **A** versus **B**, **B** versus **C**, and so on). Blocks of trials comparing the same pair of items were presented until the percentage of correct responses was at least 80% for the pair. This first step of the learning procedure was followed by a *consolidation* block (50 trials blocks repeated until performance > chance level), in which all adjacent pairs were randomly presented in the same block.

Each monkey was tested, respectively, in 6 (Monkey 1) and 4 (Monkey 2) sessions with the chain-linking procedure and in 1 and 3 sessions with the sequential learning procedure.

In the test phase (the same for both learning procedures), all possible combinations of the items (both learned pairs and novel pairs) were presented in random order; each problem (i.e., selecting the target from the non-target) was presented at least 18 times (half the with higher-ranked item on the left and half on the right).

To account for the different number of trials in the different SDists in two sessions of each monkey we balanced the number of trials in the different SDists by increasing the number of trials in the pairs comparisons at higher SDists. In these sessions the number of trials for each SDist was on average 72 (SD = 6). The two different versions of the task (balanced versus unbalanced) did not significantly affect the performance of the monkeys. A 2-way ANOVA (session type X SDist) revealed no significant differences between session types $F(1,12) = 4.44$; $p > 0.05$ or significant interactions $F(4,48) = 0.77$; $p > 0.05$. We only detected a significant main SDist effect $F(4,48) = 32.4$; $p < 0.001$.

QUANTIFICATION AND STATISTICAL ANALYSIS

Behavioral data

We evaluated the performance in each session with regard to the effect of SDist and the spatial location of the target item. To this end, for each pair of items presented, we calculated the probability to select the item on the right and left position of the screen depending on its SDdist from the non-target item. SDists for the position of the target on the left side of the screen are indicated as negative (Figures 1C and 1D). The reaction time of correct trials, calculated as the time between the Go-signal and the hand movement, was computed for each SDist. By a regression analysis, we tested if the performance increased and the reaction time decreased with the growing of SDist.

As a control analysis of the possible association between symbols and reward history during learning we tested the performance of the monkeys at the end of the chain-linking learning procedure. In this learning condition, the presentation of the C versus D pair required the monkeys to quickly rearrange the provisional representations (A > B > C and D > E > F) according to the new information (C > D): all of the values of the elements on the second list had to be revised, and new relationships among the overall items had to be formed, regardless of their relative ranks in their initially trained lists (Brunamonti et al., 2016; Treichler and Raghanti, 2010; Treichler et al., 2003).

If the entire mechanism relies on associative learning, then it should not be possible to predict a SDist effect on the unified list. In this perspective, what we call SDist effect (and logical inference) is nothing but a value transfer from the always-rewarded or never-rewarded item to the adjacent element in the list (von Fersen et al., 1991). Our results show that the SDist effect was still present in the chain-learning sessions (Figure S1B).

As further evidence of the use of a mental model for making decisions, we assessed if the SDist effect modulated the performance of both monkeys in comparing separately each item with any of the others. By means of linear regressions analyses, we tested if the rising of items' symbolic distance increased the performance and decreased the reaction time (Figure S1C).

Neural data

A pool of 186 isolated neurons (59 recorded in Monkey 1, 127 in Monkey 2), selected for not being repetitively recorded over multiple sessions by the MATLAB tool provided by Fraser and colleagues (Fraser and Schwartz, 2012), was studied during the test phase of

the task. Specifically, we asked how the neural activity of the single neurons of the dorsal premotor cortex (PMd) encoded the target item according to both the spatial position and the rank difference from the non-target item.

t test with Bonferroni correction considering all trials (correct and wrong) was used to classify cells as task-related if the neural activity concurrent with left versus right movement differed significantly in at least one of the two epochs of analysis (pair onset, **Pair-on,** corresponding to the time from 100 to 400 ms following the pair presentation and movement onset, **Mov-on,** taken as 300 ms before the arm movement initiation; see Results).

To evaluate the intensity and the time at which the neural activity for each SDist started to differ between the right and left positions, we applied ROC analysis (receiver operating characteristic) on correct trials, which takes into account not only the differences in mean response between two conditions but also the response variability of a neuron in individual trials (Thompson et al., 1996). We derived the area under the ROC (auROC), which represents the probability with which, on the basis of firing rates, the neuron can reliably identify the location of the target item in the presence of a non-target item. A value of 0.5 indicates that responses were not influenced by the target location. Conversely, a value of 1.0 or 0 indicates that responses to the target were always greater at the left or right location (arbitrarily), respectively. For each task-related neuron, the number of correct trials for the left and right presentation of the target item was equalized across each SDist. On average, the analysis was performed on 29 (SD = 17) trials for each SDist.

Spike density function of each trial was calculated by convolving the neuronal activity with exponential functions that resembled a postsynaptic potential (Thompson et al., 1996). ROC values were obtained for each consecutive time window (20 ms duration), starting 100 ms before to 800 ms after the pairs' onset.

The latency of discrimination for the target in the preferred location was defined by convention as the time when the auROC value exceeded the criterion of 0.6 or dropped below the value 0.4 for at least 3 consecutive bins 60 ms. For each neuron that reached the discrimination threshold at SDist 5 (the best discriminative condition according to the behavioral performance), we tested if the discrimination threshold was still reached at an SDist other than 5 and with comparable times. For each neuron and SDist, we also calculated the mean ROC value in the 800 ms following the pair onset to quantify the magnitude of discrimination of the target in the preferred position, regardless if it was in the left or the right position. By a Kruskal-Wallis test we evaluated, if across all neurons, the ROC significantly differed among the different SDists.

Population analysis using PCA

Population encoding of the target item selection was studied by a principal component analysis (PCA) approach. Before PCA application, neuronal data were preprocessed as reported in Yu et al. (2009). In detail, for each trial (both correct and error trials), neuronal activity from the 200 ms preceding the pair presentation time to 2200 ms following it was binned every 20 ms. Binned activity was first square-rooted and then smoothed by a Gaussian filter of 40 ms. For each neuron, we computed the mean of the smoothed activity for the position of the target item (left or right) for each of the five SDists. PCA was then applied to this main activity. Since by definition the number of trials in the unbalanced sessions was higher in the lower SDists than in higher SDists, the average neuronal activity for lower SDists was calculated on the number of trials comparable to that of higher SDists, of the population of 59 neurons recorded from Monkey 1 and the population of the 127 neurons recorded from Monkey 2. The activity of the neuronal population was then represented as a moving point within the 15-dimensional state-space of the PCs. We studied if the behavioral performance was reflected in the kinematics of the point. We first used a 4^{th}-degree polynomial function to model the projection of the neuronal activity on each of the 15 components, then we controlled for the parallelism of the different trajectories in 15 dimensions for the 5 SDists, separately for the left and right position of the target. To this end, we estimated the time evolution (−100 ms to 1400 ms from the presentation of the stimuli; 20 ms time bins) of the degree of parallelism in all pairs of trajectories (SDist1 versus SDist 2; SDist1 versus SDist 3; SDist1 versus SDist 4; SDist1 versus SDist 5; SDist2 versus SDist 3; SDist2 versus SDist 4; SDist2 versus SDist 5; SDist3 versus SDist 4; SDist 3 versus SDist 5; SDist4 versus SDist 5) as the angle of separation of pairs of points belonging to two different trajectories, respect to the origin in the state space.

Naming i, j two points in the 15-dimensional space and Vi, Vj the vectors that identify i and j with respect to the origin, the angle θ between Vi and Vj is given by:

$$\theta = arccos \frac{Vi \times Vj}{|Vi| \times |Vj|}$$

Where $||$ indicates the module. We used a Kruskal-Wallis non-parametric test to evaluate significant differences between the θ angles (factor time bins) in the full trial and Bonferroni post hoc comparisons to test if θ differed between pairs of time points following the target discrimination time to the onset of movement.

Once assessed that the different trajectories did not deviate significantly from a parallel pathway, we derived the polynomial model over time to calculate the instant velocity (V) of the moving point on each of the principal components of the space as follows:

$$V = (Vx_1, Vx_2, \ldots, Vx_{15})$$

where Vx_1, Vx_2, …, Vx_{15} are the velocities of the point in each of the 15 components calculated as:

$$Vx_1 = d(X_1)/dt, Vx_2 = d(X_2)/dt, \ldots, Vx_{15} = d(X_{15})/dt,$$

where $d(X_i)$ is the derivate of the component X_i over time.

The module of the instant velocity

$$V(t) = sqrt\left(Vx_1^2 + Vx_2^2 + \ldots Vx_{15}^2\right)$$

of the point in the 15-dimension space was compared across the trajectories of the neuronal activity in the different task conditions.

MATLAB toolboxes for statistical comparisons, data reduction (*PCA*), polynomial fitting (*polyfit*), and polynomial derivation (*polyder*) were used for data analysis.

Cell Reports, Volume *32*

Supplemental Information

Dorsal Premotor Cortex Neurons Signal the Level of Choice Difficulty during Logical Decisions

Valentina Mione, Emiliano Brunamonti, Pierpaolo Pani, Aldo Genovesio, and Stefano Ferraina

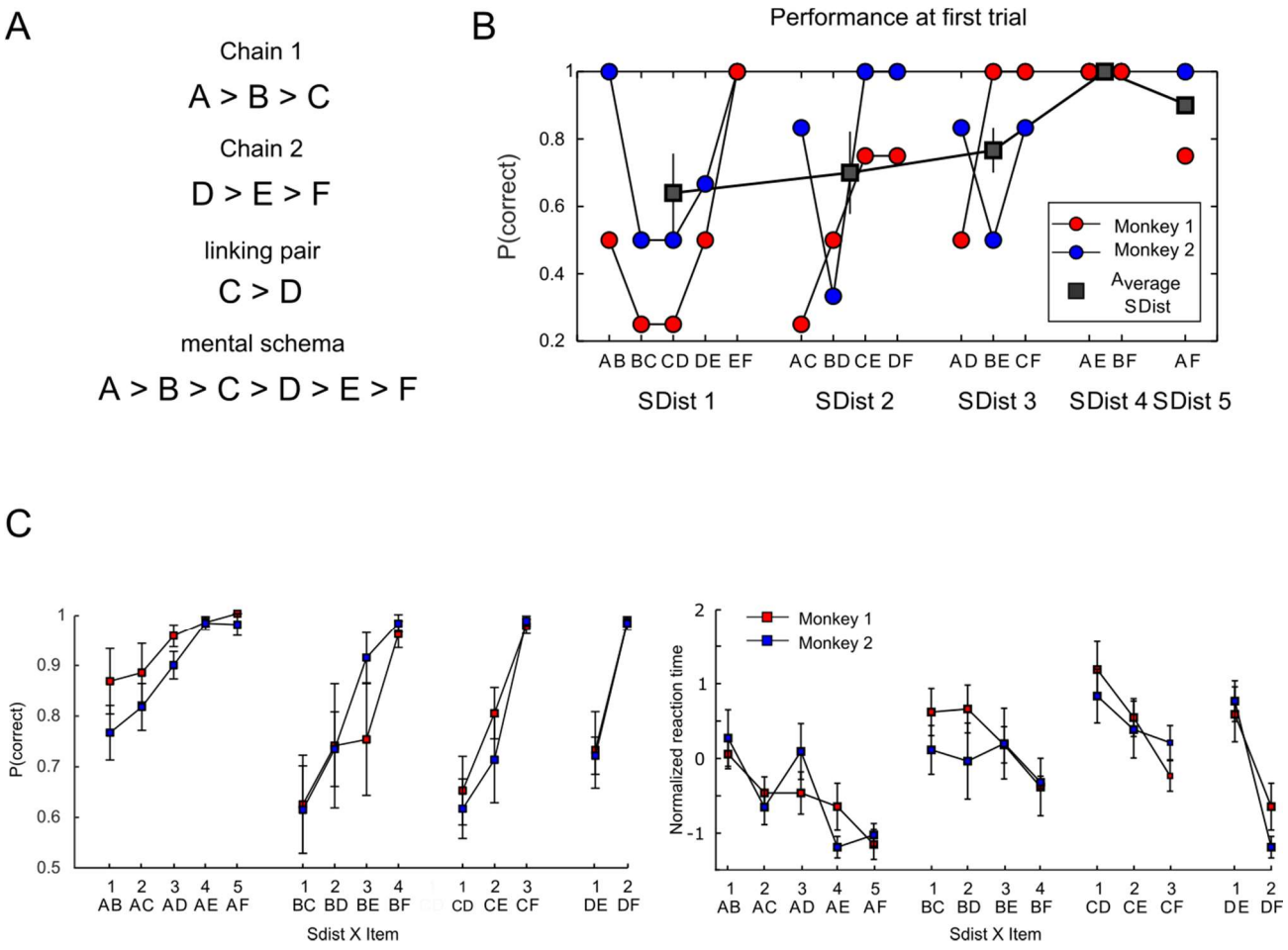

Figure S1.

Performance in transitive inference task in sessions with chain-linking learning procedure and test of SDist effect for separate item. Related to Figure 1

(A) Schematic of serial chain-linking learning. The two separate lists A>B>C and D>E>F are learned separately, and then linked by the C>D during training, in order to create a unified list A>B>C>D>E>F for controlling the reward value of the extremes items A, C, D and F. (B) Performance of both monkeys in each pair comparison (blue and red dots) at the very first trial of the test phase, after completion of learning. Since the beginning of the test phase both monkeys displayed a significant distance effect overall comparisons (black square; chi-square test (1,4) = 11.813, p = 0.019), supporting the view of the use of a mental schema driven performance. (C) Performance and normalized reaction time (RT) in comparing separately each item with all others at different symbolic distances (SDist). Error bars indicate S.E.M. A significant symbolic distance (regression line) effect emerged in all comparisons (with the exception of RT comparisons for item C and D in monkey 2). [P(correct). Monkey 1; item A: $p<0.01$; item B: $p<0.05$; item C: $p<0.001$; item D: $p<0.001$; Monkey 2: item A: $p<0.001$; item B: $p<0.001$; item C: $p<0.001$; item D: $p<0.00$] (Reaction time: Monkey 1: item A: $p<0.01$; item B: $p<0.05$; item C: $p<0.001$; item D: $p<0.001$; Monkey 2; item A: $p<0.01$; item B: $p>0.05$; item C: $p>0.05$; item D: $p<0.01$). Looking at the performance of pairs involving the highest in rank item A (left panel), it is clear how the only presence of the target item - even if stored as always-winning - is not sufficient to have a 100% rate of successful choices: the probability of success is instead modulated by the SDist, from the paired loser item. The SDist effect on a single item, then, supports the hypothesis that the degree of similarity between ranks of two items, and likely the degree of overlapping of their mental representations, modulated the difficulty in choosing one of the two symbols as the target item.

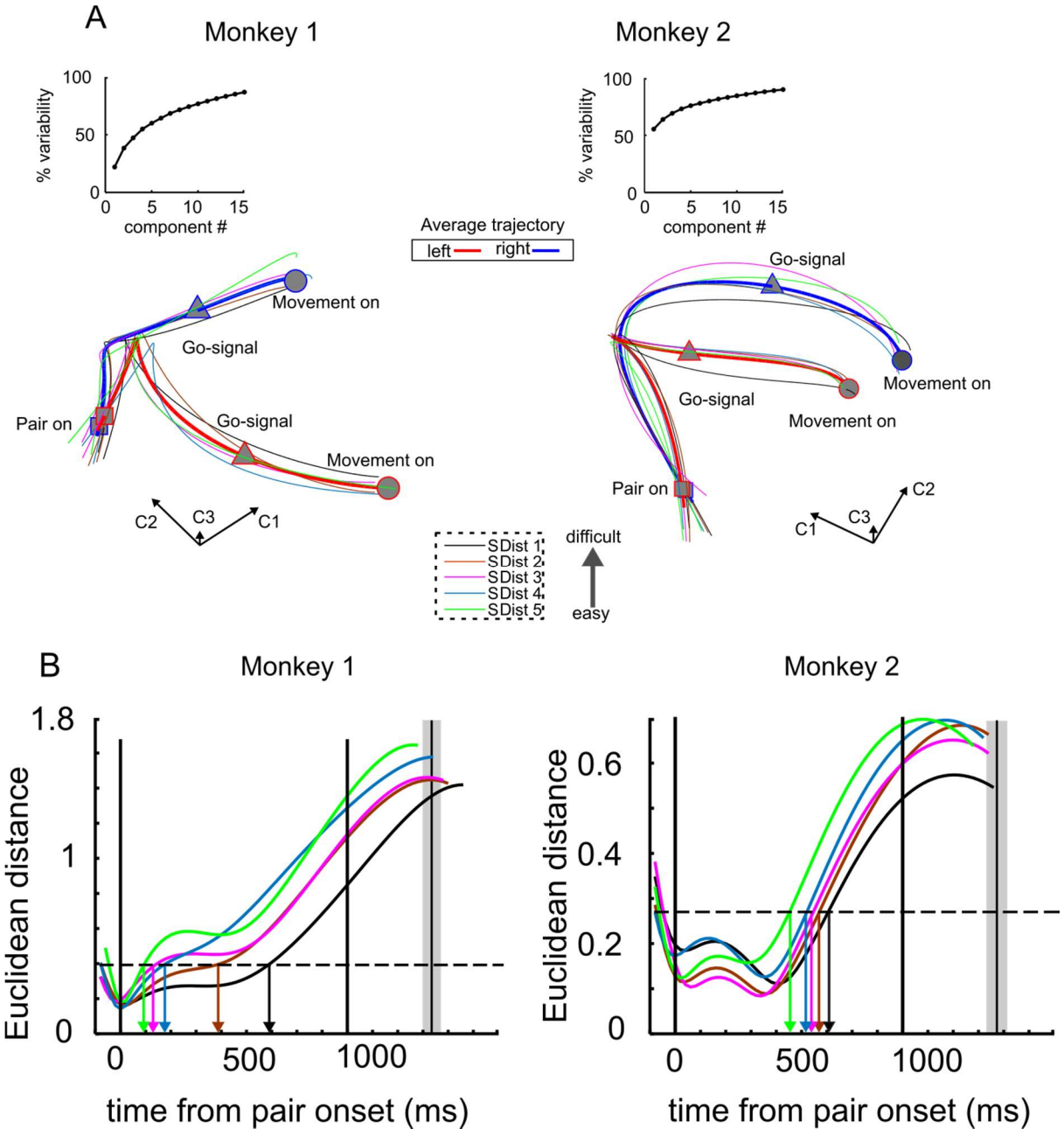

Figure S2

Population dynamics in transitive inference task in sessions with chain-linking learning procedure. **Related to Figure 3**

(A) State space dynamics of the neuronal activity in sessions with chain-linking learning in both monkeys. (B) Time evolution of the Euclidean distance between the right and left neural trajectory and instant velocity of trajectories at each SDist in the chain-linking learning sessions.

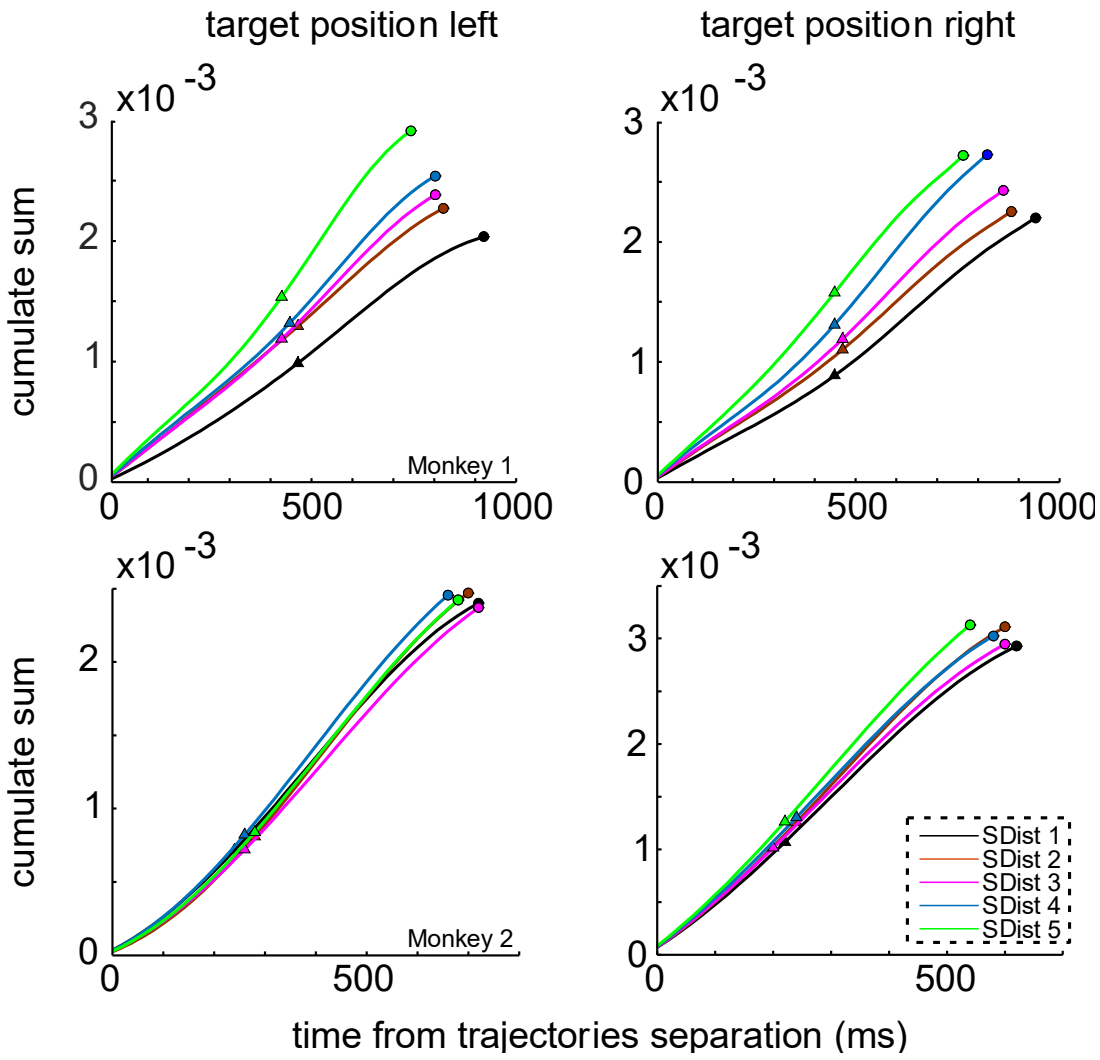

Figure S3

Network dynamics from the neuronal decision time to movement onset in chain-linking learning sessions. Related to Figure 4

In both monkeys the slope of cumulative sum of the instant velocity, in fact, was higher for higher SDist : monkey 1 left: SDist 1 = 0.06 x 10^{-3}, SDist 2= 0.07x 10^{-3}, SDist 3 = 0.088 x 10^{-3}, SDist 4 = 0.09 x 10^{-3}, SDist 5 = 0.11 x 10^{-3}; p< 0.0001; monkey 1 right: SDist 1 = 0.06 x 10^{-3}, SDist 2= 0.07 x 10^{-3}, SDist 3 = 0.08 x 10^{-3}, SDist 4 = 0.09 x 10^{-3}, SDist 5 = 0.10 x 10^{-3}; p= 0.0001; monkey 2 left: SDist 1 = 0.07 x 10^{-3}, SDist 2= 0.08 x 10^{-3}, SDist 3 = 0.07 x 10^{-3}, SDist 4 = 0.08 x 10^{-3}, SDist 5 = 0.08 x 10^{-3}; p< 0.0001; monkey 2 right: SDist 1 = 0.09 x 10^{-3}, SDist 2= 0.10 x 10^{-3}, SDist 3 = 0.09 x 10^{-3}, SDist 4 = 0.010 x 10^{-3}, SDist 5 = 0.11 x 10^{-3}; p<0.0001).

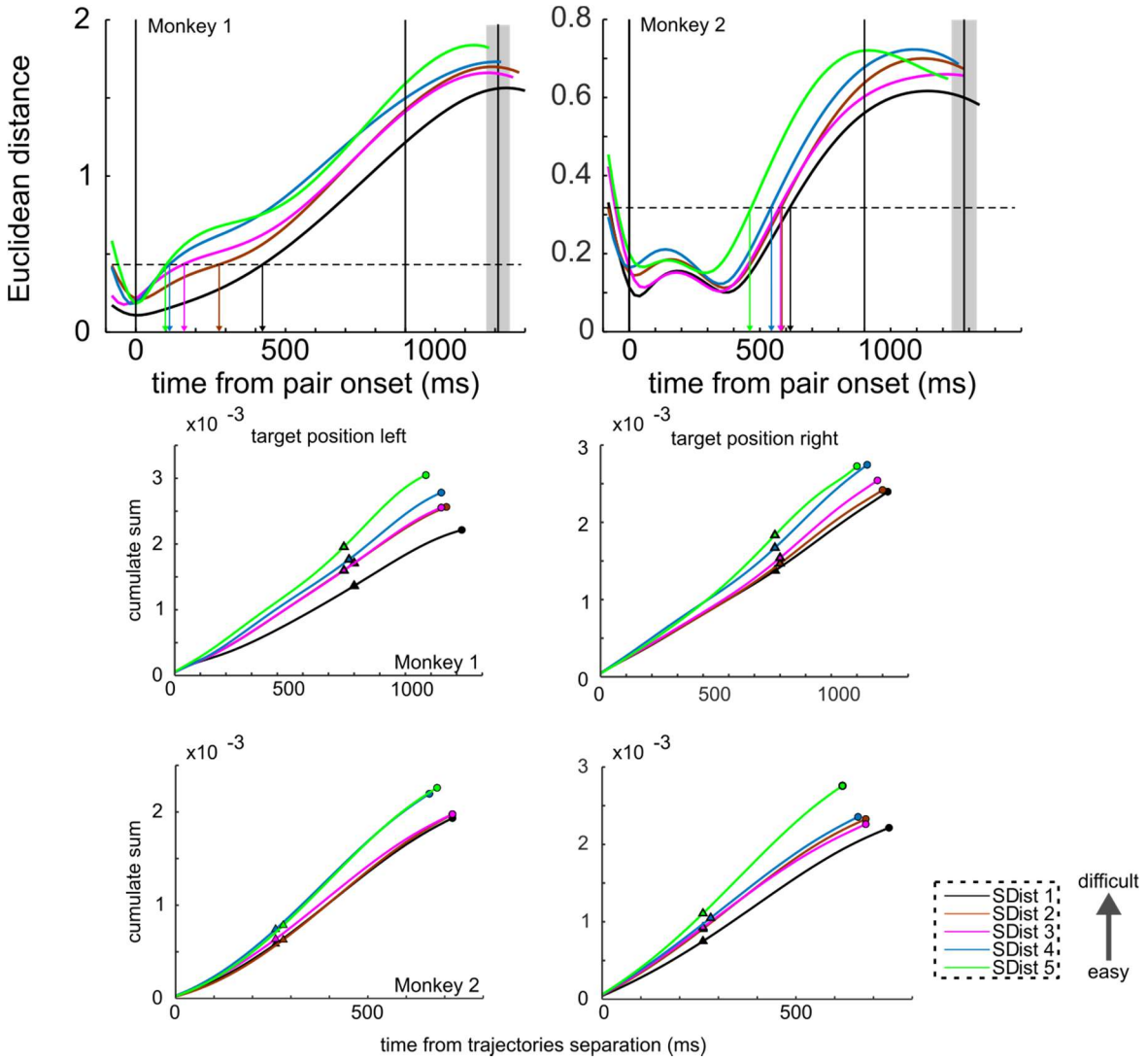

Figure S4 Population dynamics calculated for SDist modulated neurons. Related to Figures 3-4
Time evolution of the Euclidean distance for the trajectories in the state space of the 82 neurons (41 in each monkey) modulated by the SDist in the ROC analysis (see Figure 2C). The top panels reveal that in both monkeys the Euclidean distance crossed the criterion threshold with a time comparable with the decreasing of difficulty in performing the task (colored vertical arrows). Accordingly, the slopes of the cumulate distribution of velocity (bottom panels) gradually increased as the difficulty of the task decreased (Monkey 1 left target from SDist1 to SDist5 = 0.041 x 10^{-3}, 0.050 x 10^{-3}, 0.051 x 10^{-3}, 0.055 x 10^{-3}, 0.063 x 10^{-3}; right target from SDist1 to SDist5 = 0.042 x 10^{-3}, 0.044 x 10^{-3}, 0.047 x 10^{-3},0 052 x 10^{-3}, 0.056 x 10^{-3}; Monkey 2 left target SDist1-SDist5 = 0.053 x 10^{-3}, 0.054 x 10^{-3}, 0.054 x 10^{-3}, 0.065 x 10^{-3}, 0.066 x 10^{-3}; right target SDist1-SDist5 = 0.059 x 10^{-3}, 0.067 x 10^{-3}, 0.064 x 10^{-3},0 068 x 10^{-3}, 0.084 x 10^{-3}). For both monkeys, the increasing of the slope was significant for both the positions of the target (all ps<0.001).

Table S1: Regression analysis results. Related to Figure 1

	Linear regression	Linear regression
	P(select the target) – (Left target)	P(select the target) – (Right target)
Monkey 1	Y_{Left} = -0.058(SDist) + 0.73, P<0.01	Y_{Rigth} = 0.057(SDist) + 0.73, P<0.01
Monkey 2	Y_{Left} = -0.072(SDist) + 0.67, P<0.01	Y_{Rigth} = 0.069(SDist) + 0.68, P<0.01)
	Reaction Time – (Left target)	Reaction Time – (Right target)
Monkey 1	Y_{Left} = 26(SDist) + 296, P<0.01	Y_{Rigth} = -36(SDist) + 505, P<0.001
Monkey 2	Y_{Left} = 28(SDist) + 347, P<0.001	Y_{Rigth} = -31(SDist) + 505, P<0.05

Table S2. Slope of regression lines. Related to Figure 4

	Symbolic distance	Target left	Target right
Monkey 1	SDist 1	0.07×10^{-3}	0.07×10^{-3}
	SDist 2	0.08×10^{-3}	0.08×10^{-3}
	SDist 3	0.09×10^{-3}	0.09×10^{-3}
	SDist 4	0.10×10^{-3}	0.10×10^{-3}
	SDist 5	0.12×10^{-3}	0.12×10^{-3}
	P	<0.0001	<0.0001
Monkey 2	SDist 1	0.08×10^{-3}	0.09×10^{-3}
	SDist 2	0.08×10^{-3}	0.10×10^{-3}
	SDist 3	0.09×10^{-3}	0.09×10^{-3}
	SDist 4	0.10×10^{-3}	0.11×10^{-3}
	SDist 5	0.10×10^{-3}	0.13×10^{-3}
	P	<0.0001	<0.0001